Molecular Human Reproduction, Vol.25, No.3 pp. 124–136, 2019
Advanced Access publication on January 25, 2019 doi:10.1093/molehr/gay054

molecular human reproduction

ORIGINAL ARTICLE

Gonadotrophin-mediated miRNA expression in testis at onset of puberty in rhesus monkey: predictions on regulation of thyroid hormone activity and DLK1-DIO3 locus

Paula Aliberti[1], Rahil Sethi[2], Alicia Belgorosky[1], Uma R. Chandran[2], Tony M. Plant[3], and William H. Walker [3,*]

[1]Endocrine Service, Hospital de Pediatría Garrahan, Combate de los Pozos 1881(C 1245 AAM) C.A.B.A., Buenos Aires, Argentina [2]Department of Biomedical Informatics, University of Pittsburgh Cancer Institute, 5607 Baum Boulevard, Suite 500, Pittsburgh, PA 15206, USA [3]Department of Obstetrics, Gynecology and Reproductive Sciences, University of Pittsburgh School of Medicine and Magee-Womens Research Institute, 204 Craft Avenue, Pittsburgh, PA 15213, USA

*Correspondence address. E-mail: walkerw@pitt.edu orcid.org/0000-0002-5894-1239

Submitted on August 9, 2018; resubmitted on November 30, 2018; editorial decision on December 7, 2018; accepted on December 20, 2018

Molecular mechanisms responsible for the initiation of primate spermatogenesis remain poorly characterized. Previously, 48 h stimulation of the testes of three juvenile rhesus monkeys with pulsatile LH and FSH resulted in down-regulation of a cohort of genes recognized to favor spermatogonia stem cell renewal. This change in genetic landscape occurred in concert with amplification of Sertoli cell proliferation and the commitment of undifferentiated spermatogonia to differentiate. In this report, the non-protein coding small RNA transcriptomes of the same testes were characterized using RNA sequencing: 537 mature micro-RNAs (miRNAs), 322 small nucleolar RNAs (snoRNAs) and 49 small nuclear RNAs (snRNAs) were identified. Pathway analysis of the 20 most highly expressed miRNAs suggested that these transcripts contribute to limiting the proliferation of the primate Sertoli cell during juvenile development. Gonadotrophin treatment resulted in differential expression of 35 miRNAs, 12 snoRNAs and four snRNA transcripts. Ten differentially expressed miRNAs were derived from the imprinted delta-like homolog 1-iodothyronine deiodinase 3 (*DLK1-DIO3*) locus that is linked to stem cell fate decisions. Four gonadotrophin-regulated expressed miRNAs were predicted to trigger a local increase in thyroid hormone activity within the juvenile testis. The latter finding leads us to predict that, in primates, a gonadotrophin-induced selective increase in testicular thyroid hormone activity, together with the established increase in androgen levels, at the onset of puberty is necessary for the normal timing of Sertoli cell maturation, and therefore initiation of spermatogenesis. Further examination of this hypothesis requires that peripubertal changes in thyroid hormone activity of the testis of a representative higher primate be determined empirically.

Key words: Adark and Apale spermatogonia / differentiation / FSH / LH / thyroid hormone action / DIO2 / SNORD / RNA sequencing / transcriptome / spermatogonial stem cell

Introduction

In higher primates, the pituitary–testicular axis of the juvenile prior to the onset of puberty is characterized by low circulating concentrations of gonadotrophin and androgen and relative testicular quiescence (Plant *et al.*, 2005). At this stage of development, the seminiferous cords in the testis of the rhesus monkey contain only Sertoli cells and undifferentiated Type A spermatogonia (Plant *et al.*, 2005). The key event underlying the initiation of spermatogenesis at puberty in this species is a gonadotrophin-induced commitment by Type A spermatogonia to differentiate into B spermatogonia (the first generation of differentiating spermatogonia in primates). In a recent study, we prematurely elicited this critical step in spermatogonial differentiation by stimulating the testis of the juvenile monkey with exogenous LH and FSH, administered as i.v. infusions for up to 96 h (Ramaswamy *et al.*, 2017). At the termination of the infusions, total RNA was extracted from one testis for RNA sequencing (RNA-Seq) using an Illumina platform, while the other testis was fixed for morphometric and immunofluorescence analyses. As predicted, this gonadotrophin stimulation of the juvenile monkey testis resulted in Type A spermatogonia committing to a path of differentiation and Sertoli cells increasing their rate of

proliferation as reflected by bromodeoxyuridine incorporation. Interestingly, the gonadotrophin-dependent generation of differentiating B spermatogonia occurred without detectable up-regulation in the expression of mRNAs known to encode proteins that induce spermatogonia differentiation. However, the expression of genes that have been recognized in rodents to promote the maintenance of spermatogonial stem cell properties ('stemness') decreased (Ramaswamy *et al.*, 2017).

Although the earlier study described above analyzed only mRNA, there is evidence in the mouse that some micro-RNAs (miRNAs) are also involved in the determination of spermatogonial stem cell fate (Niu *et al.*, 2011; Yang *et al.*, 2013). For this reason, we took the opportunity to utilize the previously isolated testicular RNA to determine the landscape of miRNAs and other small RNAs in the testis of the juvenile monkey, and to examine the effect of gonadotrophin stimulation on the expression of these small RNAs. For this purpose, RNA-Seq with an Ion Torrent platform was used, and miRNAs were mapped to the RheMac2 reference genome because, at the time of our analysis, this reference genome was used by software annotating rhesus monkey miRNAs.

The most highly expressed miRNAs in the vehicle-treated juvenile monkey were cataloged, their functional significance explored, and the miRNAs and other small RNAs that were differentially expressed in the testis after gonadotrophin stimulation for 48 h were identified. The delta-like homolog 1-iodothyronine deiodinase 3 (*DLK1-DIO3*) and Prader–Willi imprinted regions were found to be major sources of gonadotrophin-regulated miRNAs and small nucleolar RNAs (snoRNAs), C/D box (SNORD) family, respectively. Additionally, we propose the idea that at the time of puberty in the male monkey, and likely in other higher primates, gonadotrophin-regulated miRNAs play a role in triggering an increase in thyroid hormone action in the juvenile testis; a change in local hormonal status that would likely contribute to Sertoli cell maturation and initiation of spermatogonial differentiation.

Materials and Methods

Animals

Testicular RNA from the six juvenile male rhesus monkeys (14–24 months of age; 2.3–3.3 kg body weight) that were employed in our recent study to examine the effects of 48 h of gonadotrophin stimulation on the expression of protein coding genes was used (Ramaswamy *et al.*, 2017). Three of the monkeys had received a pulsatile infusion of recombinant monkey LH and FSH (1 and 60 ng/kg/pulse, respectively, given as in i.v. bolus once every 3 h for 48 h), and three had been treated with vehicle (sterile Dulbecco's PBS). As previously described, the animals were maintained in accordance with the National Institutes of Health guidelines for the Care and Use of Laboratory Animals and the experiments were approved by the University of Pittsburgh Institutional Animal Care and Use Committee.

RNA-Seq and bioinformatics

Total RNA had been isolated from the entire right testes of each monkey using Trizol reagent (Invitrogen, Carlsbad, CA, USA) and RNeasy columns (Qiagen, Valencia, CA, USA). Prior to library preparation, rRNA was depleted using the GeneRead rRNA Depletion Kit (Qiagen). Library preparation was performed using the Ion Total RNA-Seq kit v2 for Small RNA libraries (Life Technologies, Carlsbad, CA, USA). The RNA was size selected using the double solid phase reversible immobilization selection method to obtain a final library with fragments up to 200 bases. Yield and size distribution were assessed by fluorometric assay and a Bioanalyzer with the Small RNA Kit chip (Agilent Technologies, Santa Clara, CA, USA). RNA-Seq was performed by the Genomics Research Core at the University of Pittsburgh using the Ion Torrent platform. Sequences were trimmed with Cutadapt, and reads <16 bp were discarded. Mapping and alignment of mature miRNAs to the RheMac2 reference genome were performed with miRDeep2 (Friedlander *et al.*, 2012) that employs miRBase (Kozomara and Griffiths-Jones, 2014) to subsequently annotate precursor miRNAs. It should be noted that this reference genome was derived from a female monkey, and therefore, information for miRNAs on the Y chromosome was not available. For other small RNAs, reads were aligned to an alternative rhesus monkey reference genome, RheMac8, using Bowtie v1.1.2 (Langmead *et al.*, 2009) and settings from miRDeep2 mapper. Read counts of small RNAs were generated using HTSeq (Anders *et al.*, 2015), and annotations were derived from ENSEMBL database v88.

Analysis of expression of mature miRNAs and other small RNAs

Differential gene expression analysis was performed for mature miRNAs and all other small RNAs with edgeR (Robinson *et al.*, 2010) having an initial filter that required any three of the six samples to have counts per million (CPM) >1 to allow a gene to be eligible for inclusion in the transcriptome. Differentially regulated miRNAs were defined as those in which the mean CPM values for the vehicle- and gonadotrophin-treated groups had fold changes of ≥1.5 or ≤0.5 and *p*-values <0.05. Statistical analysis of differentially expressed miRNAs was performed with an exact test based on a quantile-adjusted conditional maximum likelihood method for experiments with single factor.

Reverse transcription of RNA was performed using the miScript RT kit (Qiagen) according to manufacturer's directions with 100 ng of RNA. Real-time quantitative PCRs (qPCRs) included 1 µl of a 1:20 dilution of reverse transcription reaction, 1 µl each of 10 mM stocks of primers, 6 µl of water and 10 µl of PerfeCTa Sybr Green Super Mix (Quantabio, Beverly, MA, USA). A reverse primer (universal short reverse) complimentary to the 5′ end of the reverse transcription primer was used for all amplification reactions with specific forward primers complimentary to the 5′ region of each miRNA. Primer pairs were independently validated for use in the ΔΔCt method of gene expression analysis (Bookout *et al.*, 2006) through use of a standard curve derived from serial dilutions of the cDNA obtained from the reverse transcription reactions. Primers with an efficiency of 2 ± 0.2 were considered acceptable. snoRNAs, C/D box 27 (SNORD27), which RNA-Seq analysis found varied <0.1-fold after gonadotrophin stimulation, was used as an endogenous control for normalization. The qPCRs were performed and analyzed as described previously (Wood *et al.*, 2011). Dissociation curve analysis was performed after amplification. The list of primers used is presented in Supplementary Table S1.

Identification of potential targets of highly expressed and differentially expressed miRNAs

mRNA targets for the 20 most highly expressed miRNAs were identified from the *Homo sapiens* dataset list of experimentally observed targets using ingenuity pathway analysis (IPA; Qiagen). The functions associated with the target mRNAs were identified from the IPA options: (1) molecular and cellular functions and (2) physiological system development and function, with *p*-value <0.05 for right-tailed Fisher's exact test after the application of Benjamini–Hochberg (B–H) method of multiple testing correction.

mRNA targets for up- and down-regulated miRNAs were identified using IPA from the list of juvenile monkey testis genes that were previously found to be down- or up-regulated, after gonadotrophin stimulation (Ramaswamy *et al.*, 2017). Potential mRNA targets were accepted from the following

three IPA categories: experimentally observed, highly predicted and moderately predicted. In the few cases when IPA failed to predict the miRNA targets, TargetScan (v7.0) was used to find potential targets using a context++ score (defined at http://www.targetscan.org/vert_70/docs/context_score_totals.html) (Agarwal *et al.*, 2015) of ≤0.1 as a threshold. The threshold chosen was based on the gene with the highest (worst) context++ score derived from a TargetScan analysis of IPA identified targets. To determine their potential functional significance, the list of target mRNAs was analyzed by IPA to identify over-represented categories of ingenuity canonical pathways with *p*-values <0.05, as described earlier.

Characterization of the DLK1-DIO3 domain in the rhesus monkey

A major cohort of miRNAs was found to be derived from genes within the imprinted *DLK1-DIO3* locus of chromosome 7. Because the *DLK1-DIO3* locus of the monkey was poorly annotated in RheMac2, an attempt was made to better characterize this genomic region of interest by incorporating information from an alternative rhesus reference genome (RheMac8) and the more fully annotated human reference genome, GRCh28. The location of genes encoding long non-coding RNAs (lncRNAs), as well as differentially methylated regions (DMRs) or CpG enriched regions that were not annotated in the RheMac2 reference genome were inferred by identifying the position of the corresponding gene in RheMac8 or GRCh28. The location of the unannotated gene or sequence was then assigned the corresponding position within RheMac2. The locations of unannotated lncRNA genes were confirmed by using Integrative Genome Viewer software (Robinson *et al.*, 2011) to search for corresponding transcripts in the GEO-NCBI repository (GSE97786) derived from the unfiltered database generated in our earlier study (Ramaswamy *et al.*, 2017). Lastly, the identities of unannotated genes were confirmed by using a BLAST strategy to compare transcript sequences. A value of <0.05 was considered statistically significant.

Results

The testicular miRNA transcriptome of the juvenile monkey and the impact of gonadotrophin stimulation

RNA-Seq analysis identified 537 mature miRNAs in the testes of the vehicle-treated juvenile monkeys (Supplementary Table SII). Although genes expressing miRNAs were present on all autosomes and the X chromosome, 41% were expressed from three chromosomes; 7, 19 and X (Fig. 1). Of the mature miRNAs in the miRNA testicular transcriptome, 523 also were expressed in the testes that had been stimulated with LH and FSH for 48 h; an additional 29 mature miRNAs were expressed after gonadotrophin stimulation (Supplementary Table SII), but only one of these (miR-7182-3p) fulfilled the requirement to be classified as a differentially expressed (see below).

The 20 most highly expressed mature miRNAs in the vehicle-treated testes are shown in Fig. 2A. Three members of the Lethal-7 (let-7) gene family and four members of the miR-10 family were represented in this cohort of transcripts. Gonadotrophin stimulation did not influence the composition of the 20 most highly expressed miRNA genes, and none of the transcripts in this cohort were differentially expressed (Fig. 2A).

Target and pathway analysis using IPA software indicated that the 20 most highly expressed miRNAs in the transcriptome could potentially target a combined 527 mRNAs. Further analysis revealed that the potential target mRNAs were associated with 36 molecular and cellular function networks with corrected *p*-values better than 2.55×10^{-16} (Supplementary Table SIII). The 20 networks having the most significant *p*-values included those related to cell survival, proliferation, development and migration (Fig. 2B).

Differentially expressed miRNAs induced by gonadotrophin stimulation

Gonadotrophin treatment for 48 h resulted in the differential expression of 35 mature miRNAs, of which 21 were up-regulated and 14 were down-regulated (Table I). Localization of each differentially expressed miRNA on their chromosome of origin is shown in Fig. 3A. Five of the differentially expressed miRNAs (14%) were derived from the X chromosome. Another 10 differentially expressed miRNAs (28%) were derived from within the imprinted *DLK1-DIO3* locus that in the rhesus monkey spans 850 kb of distal chromosome 7 (Fig. 3B): eight of these were up-regulated and expressed from the positive strand, with seven localized to two clusters of miRNAs and one (miR-370) between the clusters. One other differentially expressed miRNA gene (miR-544) present within the second miRNA cluster was down-regulated and expressed from the positive strand. An additional miRNA (miR-1247) localized just upstream of the *DIO3* at the terminus was down-regulated and expressed from the negative strand (Fig. 3). RT-qPCR analysis of

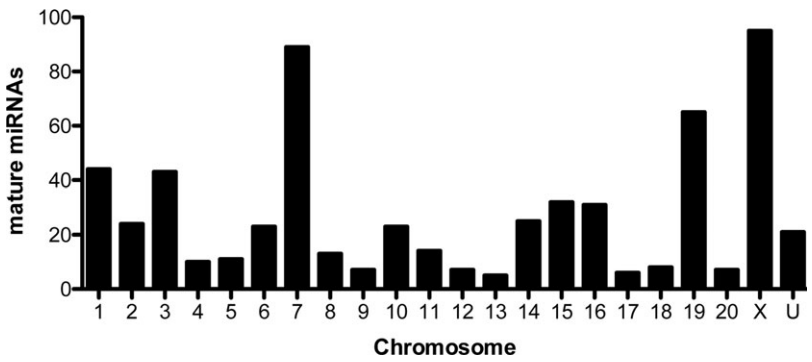

Figure 1 The chromosomal distribution of mature micro-RNAs (miRNAs) expressed by the testis of the juvenile rhesus monkey (vehicle-treated). U, mature miRNAs expressed at unannotated locations.

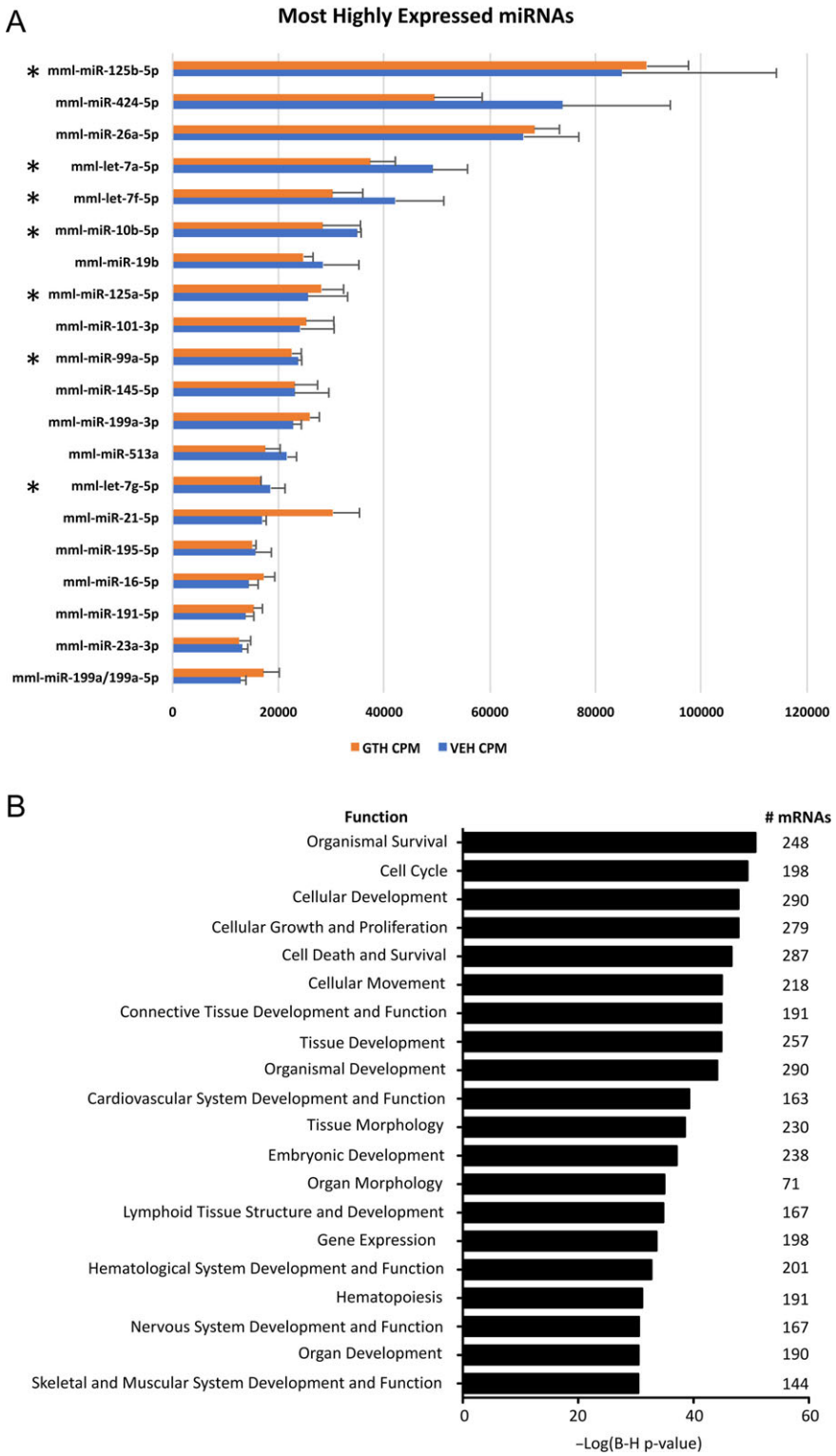

Figure 2 Expression and functional characteristics of the 20 most highly expressed mature micro-RNAs (miRNAs). (**A**) The 20 most highly expressed mature miRNAs (mean ± SEM counts per million: CPM) in the testis of juvenile monkeys treated with vehicle (Veh, blue) were not impacted by gonadotrophin stimulation (GTH, red). Members of the let-7 and MIR-10 families are marked with an asterisk (*). (**B**) Molecular and cellular functions that were over-represented among the mRNA targets of the most highly expressed miRNAs in testes of the juvenile rhesus monkey (vehicle-treated, ranked by –Log(B–H) corrected *p*-values). Categories having the 20 lowest *p*-values after Benjamini–Hochberg multiple testing correction are shown.

Table I miRNAs that are differentially expressed in juvenile monkey testes after 48 h of gonadotropin treatment.

Mature miRNA	Locus	FC	*p*-value
mml-miR-219-5p	4:32 922 221–32 922 330, 15:10 478 575–10 478 671	0.15	0.02
mml-miR-219	4:32 922 221–32 922 330, 15:10 478 575–10 478 671	0.15	0.02
mml-miR-95-5p	5:771 296–771 376	0.17	0.00
mml-miR-605	1 099 214 739 355:6911–6992	0.27	0.02
mml-miR-190a-5p	7:41 206 805–41 206 889	0.33	0.01
mml-miR-190b	1:132 712 583–132 712 661	0.35	0.04
mml-miR-450b-3p	X:132 765 568–132 765 645	0.36	0.01
mml-miR-365-3p	20:14 421 395–14 421 481, 16:26 755 289–26 755 399	0.37	0.01
mml-miR-1247-5p	**7:164 844 829–164 844 886**	**0.39**	**0.02**
mml-miR-544	**7:164 333 144–164 333 234**	**0.39**	**0.04**
mml-miR-33b-5p	16:17 718 310–17 718 405	0.40	0.05
mml-miR-190a-3p	7:41 206 805–41 206 889	0.42	0.02
mml-miR-582-5p	6:57 373 382–57 373 479	0.51	0.02
mml-miR-193a-3p	16:26 739 889–26 739 973	0.51	0.05
mml-miR-223	X:64 563 509–64 563 618	1.72	0.04
mml-miR-221-3p	X:43 559 275–43 559 384	1.78	0.04
mml-miR-494-3p	**7:164 314 563–164 314 643**	**1.82**	**0.04**
mml-miR-1260b	14:94 898 477–94 898 584	1.86	0.01
mml-miR-188-5p	X:47 638 603–47 638 688	1.95	0.02
mml-miR-484	20:15 357 361–15 357 423	2.08	0.01
mml-miR-147b	7:23 776 288–23 776 367	2.09	0.01
mml-miR-31-5p	15:55 496 756–55 496 826	2.32	0.04
mml-miR-493-3p	**7:164 153 015–164 153 103**	**2.32**	**0.02**
mml-miR-541-5p	**7:164 348 143–164 348 226**	**2.36**	**0.05**
mml-miR-485-3p	**7:164 339 347–164 339 419**	**2.37**	**0.03**
mml-miR-671-5p	3:188 187 719–188 187 836	2.38	0.00
mml-miR-675-5p	14:1 908 081–1 908 153	2.38	0.01
mml-miR-370-5p	**7:164 195 455–164 195 529**	**2.46**	**0.04**
mml-miR-1185-3p	**7:164 328 686–164 328 795, 7:164 327 486–164 327 544**	**2.72**	**0.00**
mml-miR-1271-3p	6:172 840 483–172 840 591	2.76	0.04
mml-miR-503-5p	X:132 771 696–132 771 766	3.82	0.00
mml-miR-431	**7:164 164 951–164 165 064**	**3.83**	**0.00**
mml-miR-665	**7:164 158 856–164 158 927**	**4.03**	**0.00**
mml-miR-7182-5p	2:113 620 441–113 620 502	8.87	0.00
mml-miR-7182-3p	2:113 620 441–113 620 502	28.85	0.01

Bold font denotes differentially expressed miRNAs that are localized to the delta-like homolog 1-iodothyronine deiodinase 3 (DLK1-DIO3) locus. FC = fold change after gonadotrophin treatment for 48 h. *p*-Values were generated by edgeR software that uses an exact test based on a quantile-adjusted conditional maximum likelihood method for experiments with single factor.

five differentially expressed miRNAs validated the RNA-Seq results (Supplementary Fig. S1).

Potential targets and pathways regulated by the differentially expressed miRNAs

We previously identified in the vehicle-treated testis 1587 protein encoding mRNAs that were either up-regulated or down-regulated after the 48 h of gonadotrophin stimulation (Ramaswamy *et al.*, 2017). Of these genes, 408 genes were identified as potential targets for the 35 mature miRNAs that were induced or repressed by the same LH and FSH treatment (Supplementary Table SIV). The pathways associated with the target mRNAs having the highest significance scores included those required for mitochondrial function, oxidative phosphorylation, endocytosis, and actin cytoskeleton signaling (Table II). Also, pathways including thyroid hormone, sirtuin and integrin signaling, and epithelial adherens junction formation were identified.

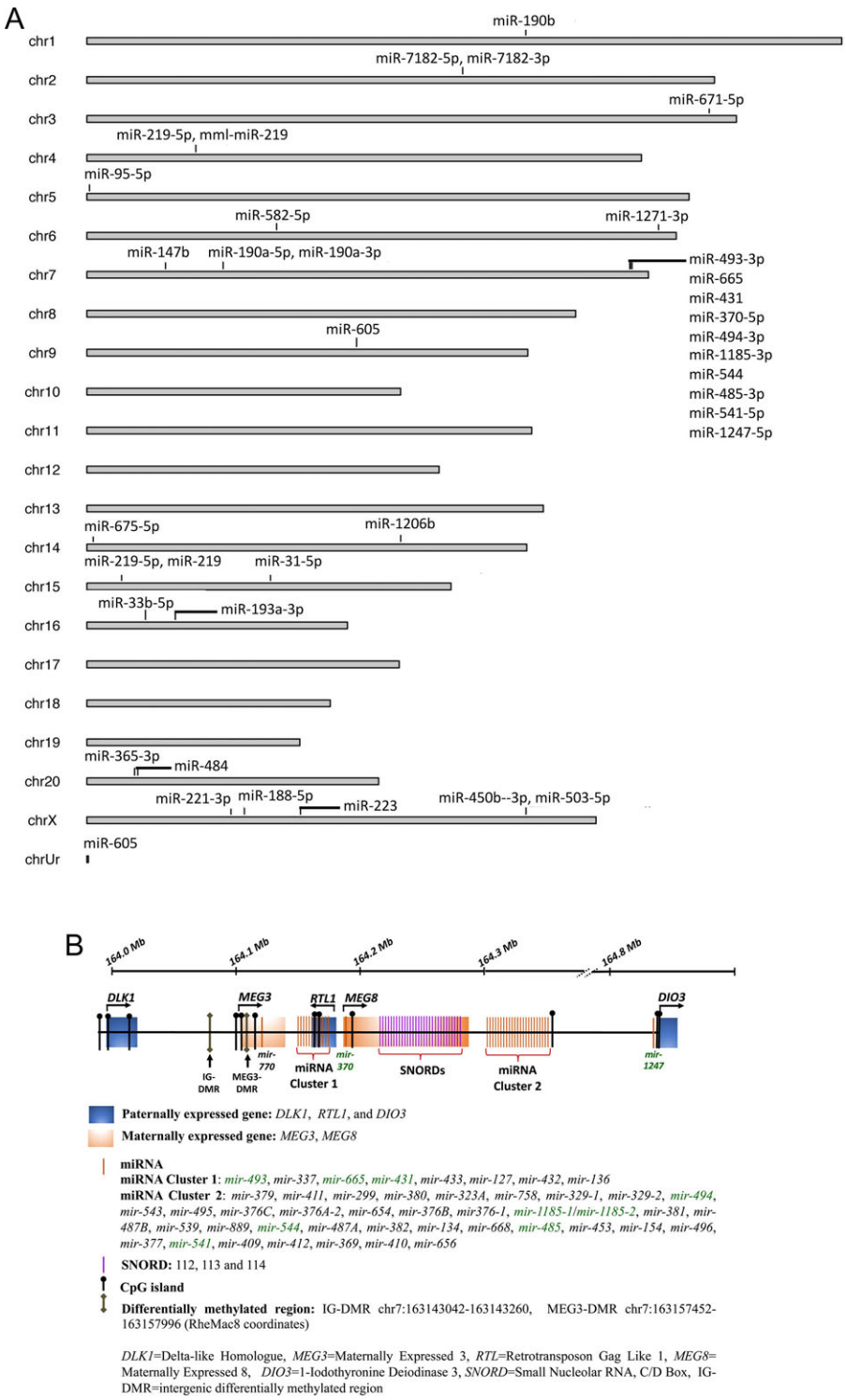

Figure 3 Localization of mature micro-RNAs (miRNAs) and other small RNAs to their chromosomal origins. (**A**) A chromosome ideogram showing the relative positioning on chromosomes of the genes encoding each mature differentially expressed miRNA (Chr Ur shows a miRNA expressed at an unannotated location). (**B**) Map of the *DLK1-DIO3* locus on chromosome 7 of the rhesus monkey. The locations of genes encoding mRNAs (*DLK1*, *RTL1*, *DIO3*), miRNAs, SNORDs and lncRNAs (MEG3, MEG8), as well as CpG islands and differentially methylated regions (DMRs) are provided. Precursor miRNAs that encode differentially expressed mature miRNAs are noted in green font. Chromosome 7 locations shown are from the RheMac2 reference genome except for DMRs as noted.

Table II Pathways associated with mRNA targets of differentially expressed miRNAs.

Ingenuity Canonical Pathways	B–H *p*-value	# target mRNAs	Target mRNAs
Mitochondrial Dysfunction	<0.01	14	COX17, PSENEN, COX6C, GPX7, ATP5E, NDUFB3, GSR, CASP9, TXN2, COX5A, COX7A2, SDHD, NDUFA12, ATP5G3
Clathrin-mediated Endocytosis Signaling	<0.01	14	FGF17, ACTR2, LDLR, ACTR3, FGF10, ARPC1B, IGF1, ACTB, ARPC5, TFRC, IRS2, ITGB8, ACTG1, FGF7
Actin Cytoskeleton Signaling	<0.01	15	ACTR2, FN1, PAK6, ARPC1B, ACTB, ARPC5, MYLK, FGF17, FGF10, ACTR3, CD14, IRS2, VCL, FGF7, ACTG1
Sirtuin Signaling Pathway	<0.01	17	PGK1, NDRG1, TIMM44, TIMM23, ESRRA, HMGCS2, ATP5E, NDUFB3, MYC, PGAM1, FOXO3, SDHD, NDUFA12, LDHA, SLC25A5, BCL2L11, TOMM5
Remodeling of Epithelial Adherens Junctions	<0.01	8	ACTR2, NME1, ACTR3, ARPC1B, ACTB, ARPC5, VCL, ACTG1
Oxidative Phosphorylation	0.013	9	COX17, COX6C, COX5A, COX7A2, SDHD, NDUFA12, ATP5G3, NDUFB3, ATP5E
Integrin Signaling	0.013	13	ACTR2, ARPC1B, PAK6, ACTB, RALB, ARPC5, MYLK, ITGA10, ITGB8, ACTR3, IRS2, VCL, ACTG1
NRF2-mediated Oxidative Stress Response	0.013	12	GSR, DNAJB11, ACTB, SLC35A2, GSTM4, IRS2, JUNB, ENC1, ACTG1, CLPP, NAJB5, PRKCB
Histidine Degradation III	0.014	3	FTCD, MTHFD2, MTHFD1
Folate Transformations I	0.019	3	MTHFD2, MTHFD1, SHMT2
Hepatic Fibrosis / Hepatic Stellate Cell Activation	0.026	11	COL9A1, FN1, IGF1, EDNRB, EDN1, CCL2, COL4A3, NGFR, IGFBP3, CD14, EDNRA
Thyronamine and Iodothyronamine Metabolism	0.031	2	DIO2, DIO3
Thyroid Hormone Metabolism I (via Deiodination)	0.031	2	DIO2, DIO3
Regulation of Actin-based Motility by Rho	0.039	7	ACTR2, ACTR3, ARPC1B, PAK6, ACTB, ARPC5, MYLK
Epithelial Adherens Junction Signaling	0.042	9	ACTR2, ACTR3, ARPC1B, ACTB, ARPC5, ACVR2B, VCL, ACTG1, ACVR1C
Fcγ Receptor-mediated Phagocytosis in Macrophages and Monocytes	0.042	7	ACTR2, ACTR3, ARPC1B, ACTB, ARPC5, ACTG1, PRKCB
fMLP Signaling in Neutrophils	0.048	8	CALM1 (includes others), ACTR2, ACTR3, ARPC1B, ARPC5, PLCB1, IRS2, PRKCB
RhoA Signaling	0.048	8	ACTR2, ACTR3, ARPC1B, IGF1, ACTB, ARPC5, MYLK, ACTG1

p-Values were determined by ingenuity pathway analysis software using a right-tailed Fisher's exact test after application of Benjamini–Hochberg (B–H) method of multiple testing correction.

Other small RNAs

Analysis of the testes from vehicle-treated juvenile monkeys identified a total of 385 small RNAs (Supplementary Table SV), the majority of which were snoRNAs (322 transcripts). In addition, there were 49 small nuclear RNA (snRNA) transcripts and 14 small Cajal body-specific RNA (scaRNA) transcripts. A further 12, 12, and two snoRNA, snRNA and scaRNA transcripts, respectively, were expressed only after gonadotrophin treatment.

Twelve snoRNA and four snRNAs transcripts were differentially expressed in the testis after gonadotrophin stimulation including six SNORDs that were localized to the imprinted Prader–Willi locus on chromosome 7 (Table III). Five copies of SNORD116 (HBII-85 in humans) that did not meet the criteria for an expressed transcript in the vehicle-treated testes, were up-regulated by 5- to 12-fold after gonadotrophin treatment. Three copies of SNORD115 (HBII-52 in humans) were down-regulated 58–74% after gonadotrophin stimulation.

Characterization of the DLK1-DIO3 domain in the rhesus monkey

Because 28% of the gonadotrophin-regulated miRNAs were expressed from the *DLK1-DIO3* locus, we focused on further characterizing this domain of the monkey genome. The lncRNA genes, *MEG3* (maternally expressed 3) and *MEG8* (maternally expressed *8*), that in other mammals flank the first miRNA cluster of this domain, were not annotated in RheMac2. Therefore, these genes were assigned locations in RheMac2 that corresponded to those in the human reference genome (MEG3) and RheMac8 (MEG8) (Fig. 3). We also mapped 18 CpG-enriched regions and two DMRs within the

Table III snoRNAs and small nuclear RNAs that are differentially expressed in juvenile monkey testes 48 h after gonadotrophin treatment.

Gene name	sRNA type	Locus	Strand	FC	p-value
SNORD33	snoRNA	19:44 875 708–44 875 792	+	0.16	<0.01
SNORD49	snoRNA	16:16 240 563–16 240 634	–	0.01	<0.01
SNORD103	snoRNA	1:30 009 980–30 010 064	–	0.35	0.03
SNORD115	snoRNA	7:2 139 675–2 139 756	+	0.26	<0.01
SNORD115	snoRNA	7:2 135 926–2 136 007	+	0.42	0.02
SNORD115	snoRNA	7:2 120 960–2 121 041	+	0.42	0.02
SNORD116	snoRNA	7:1 979 790–1 979 881	+	5.74	0.01
SNORD116	snoRNA	7:1 972 288–1 972 379	+	5.30	0.02
SNORD116	snoRNA	7:1 980 919–1 981 010	+	4.78	0.02
SNORD116	snoRNA	JSUE03317066.1:1366–1457	–	12.04	<0.01
SNORD116	snoRNA	JSUE03317066.1:224–315	–	6.13	0.01
snoU83B	snoRNA	10:81 293 316–81 293 408	–	0.37	0.02
U2	snRNA	7:74 113 310–74 113 499	+	2.18	0.04
U2	snRNA	15:102 643 508–102 643 698	–	0.37	0.04
U5	snRNA	3:77 850 907–77 851 044	+	0.37	0.02
U5	snRNA	2:102 187 939–102 188 051	+	0.18	0.03

snoRNAs: small nucleolar RNAs, snRNAs: small nuclear RNAs. *p*-Values were generated by edgeR software that uses an exact test based on a quantile-adjusted conditional maximum likelihood method for experiments with single factor.

DLK1-DIO3 domain; the latter comprised a primary, germline intergenic DMR (IG-DMR), and a secondary, somatic MEG3-DMR.

Discussion

Comparison of the testicular miRNAs identified in the present study of the juvenile monkey to those expressed by immature Sertoli cells purified from 6-day-old C57Bl/6 mouse testes (Ortogero *et al.*, 2013) revealed that of the 235 miRNAs found in the mouse Sertoli cells, 169 (72%) of the corresponding miRNAs were expressed in the testis of the vehicle-treated juvenile monkey. Moreover, 10 of the most highly expressed miRNAs in the monkey testis (let-7a, let-7f, let-7g, miR-10b, miR-125a-5p, miR-125b-5p, miR-99a, miR-26a, miR-199a-3p, miR-19b) also were in the group of the 20 most expressed miRNAs in 6-day-old mouse Sertoli cells. These findings suggest that the immature Sertoli cells are a major contributor of highly expressed miRNAs in the testis of the juvenile monkey: a view consistent with the juvenile monkey testes comprising 90% Sertoli cells (Simorangkir *et al.*, 2012; Ramaswamy *et al.*, 2017).

Pathway analysis of the 20 most highly expressed miRNAs in the juvenile monkey testis indicated that they regulate cell proliferation, survival and migration: an outcome consistent with the observation that seven of these transcripts are members of the miR-10 and let-7 miRNA families that are recognized to inhibit cell proliferation (Huang *et al.*, 2009; Jung *et al.*, 2010; Jiajie *et al.*, 2017). Although the functions of miRNAs specifically in immature Sertoli cells have not yet been characterized, it seems reasonable to propose that the highly expressed miRNAs identified in the present study contribute to maintaining the slow rate of proliferation of these cells in the monkey testis during juvenile development (Ramaswamy *et al.*, 2017). If this is indeed the case, then other cues must have been responsible for triggering the concomitant increase in mitotic activity of this somatic cell that we have previously reported (Ramaswamy *et al.*, 2017) because expression of the most abundant miRNAs was not altered after 48 h of gonadotrophin treatment. It is also possible that members of the let-7 family of miRNAs regulate the fate of undifferentiated spermatogonia in the rhesus monkey, as at least eight members of this family of miRNAs have been detected in undifferentiated Type A spermatogonia from mice (Chen *et al.*, 2017) and let-7 miRNAs are known to promote the differentiation of mouse spermatogonia stem cells by inhibiting expression of LIN28 (Rybak *et al.*, 2008).

Gonadotrophin stimulation of the juvenile monkey testis resulted in the identification of 35 miRNAs that met the criteria for differential expression, of which 15 were derived from two chromosomes, 7 and X. Chromosome 7 of the monkey contains the *DLK1-DIO3* locus, which houses the largest miRNA mega-cluster known in mammals (Seitz *et al.*, 2004; Qian *et al.*, 2016). The miRNAs encoded by the *DLK1-DIO3* locus were previously found to be associated with the pluripotency of induced pluripotent stem (iPS) cells and with regulation of self-renewal and differentiation of embryonic stem cells (Moradi *et al.*, 2017). Furthermore, increased expression of the miRNAs within the cluster has been proposed as a marker to distinguish fully pluripotent iPS cells or embryonic stem cells from partially pluripotent cells (Liu *et al.*, 2010).

As in other species, most of the genes encoding miRNAs in the *DLK1-DIO3* region in the monkey are separated into two distinct clusters; the first one between *MEG3* and Retrotransposon Gag Like 1 (*RTL1*) (cluster 1 in Fig. 3) encodes eight precursor miRNAs of which three produced differentially expressed mature miRNAs after gonadotrophin treatment, and the second more extensive cluster produces

37 precursor miRNAs (six mature miRNAs were differentially expressed) located between *MEG8* and *DIO3* (cluster 2 in Fig. 3). All the differentially expressed miRNAs in the *DLK1-DIO3* locus were up-regulated with the exception of miR-544 in the second miRNA cluster and miR-1247 that is present just upstream of *DIO3* at the terminus of the locus.

The miRNAs derived from the *DLK1-DIO3* locus of the monkey testis appear to be preferentially responsive to gonadotrophin stimulation during juvenile development because whereas 14% (74 of 537) of the mature miRNAs in the testicular transcriptome were expressed from this region, the same locus accounted for a noticeably higher proportion of differentially expressed transcripts (29%, 10 of 35). One of the differentially expressed miRNAs from the monkey *DLK1-DIO3* locus (miR-1185-3p) is not present in the miRBase database of mouse miRNAs, and of the remaining nine differentially regulated mature miRNAs from the locus, only miR-431 was detected (at the lowest of levels) in Sertoli cells purified from 6-day-old C57Bl/6 mouse testes (Ortogero *et al.*, 2013). The lack of association of the differentially expressed miRNAs from the *DLK1-DIO3* locus in the monkey with those known to be expressed in mouse Sertoli cells raises the possibility that these transcripts may be expressed in undifferentiated spermatogonia in higher primates.

DIO3, the gene that marks the terminus of the locus, encodes a type 3-iodothyronine deiodinase that degrades thyroid hormone into inactive metabolites (St Germain and Galton, 1997). A second gene involved in regulating tissue levels of thyroid hormone activity (*DIO2*) is also located on chromosome 7 but outside of the *DLK1-DIO3* locus. DIO2 generates the active form of thyroid hormone (triiodothyronine) from the circulating precursor (thyroxine). Interestingly, *DIO2* is predicted to be a target of three miRNAs (miR-450-3p, miR-544 and miR190a-3p) that were down-regulated by gonadotrophin treatment, and one of these miRNAs (miR-544) is derived from the *DLK1-DIO3* locus. *DIO3*, on the other hand, is a target of miR-484 that was induced by gonadotrophin treatment. The foregoing gonadotrophin-dependent changes in miRNA levels would be predicted to decrease *DIO3* expression and induce that of *DIO2*; a prediction that is strongly supported by our earlier RNA-Seq data showing a 70% decrease and 2.7-fold increase, respectively, in the expression of these two genes (Supplementary Table SVa in Ramaswamy *et al.*, 2017). If these changes in expression are directly related to protein levels of the thyroid hormone metabolizing enzymes, then it can be hypothesized that stimulation of the juvenile monkey testis with exogenous gonadotrophin results in a local increase in thyroid hormone activity. There is precedence for this hypothesis as it is generally recognized that expression of DIO2 and DIO3 is locally regulated to control thyroid hormone activity in other developing organs (Dentice *et al.*, 2013). Additionally, re-examination of our earlier mRNA sequence data for the same testes and for those stimulated for 96 h (Ramaswamy *et al.*, 2017) revealed that several thyroid hormone target genes were differentially expressed after gonadotrophin treatment (Supplemental Table SVI). Most notably, insulin-like growth factor 1 (*IGF1*) was up-regulated ~3-fold, whereas thyroid hormone receptor beta (*THRB*) was down-regulated by >50%. Furthermore, it follows that such a posited increase in thyroid hormone activity would take place spontaneously following the pubertal rise in pituitary LH and FSH secretion that in the monkey occurs at ~3 years of age (Plant *et al.*, 2015), i.e. when animals are 12 months or more older than those employed in the present study. An analogous situation was reported for the mouse in which the enzymatic activity of DIO3 in the testis was greatly elevated during the first 15 days of postnatal life (promoting lower thyroid hormone activity) before declining to low and stable levels in the adult (Martinez *et al.*, 2016). Although thyroid hormone levels were not measured in the present study, changes in circulating thyroxine concentrations at around the time pubertal acceleration in testicular growth is initiated in the monkey were reported to be unremarkable (Mann *et al.*, 2002), further suggesting that the posited changes in thyroid hormone activity are likely limited to the testis.

The duration of the posited low thyroid hormone activity in the testis of the pre-pubertal mouse and monkey is tightly coupled to the time course of Sertoli cell proliferation in the two species. In the rodent, Sertoli cell proliferation is elevated during the first 2 weeks of life and terminated ~21 days of age (Orth, 1982); whereas, in the monkey, proliferation continues throughout the juvenile period, a phase of development spanning ~3 years (Simorangkir *et al.*, 2012). In both species, the arrest of Sertoli cell proliferation coincides with maturation of this cell. A causal link between thyroid status and Sertoli cell maturation is suggested by the finding that, in rats, transient neonatal hyperthyroidism or hypothyroidism accelerate and retard, respectively, the differentiation of Sertoli cells (Van Haaster *et al.*, 1992; 1993; Bunick *et al.*, 1994; Rijntjes *et al.*, 2009). Also, in pubertal boys, hypothyroidism has been reported in association with macro-orchidism likely caused by increased Sertoli cell number (Castro-Magana *et al.*, 1988; Weber *et al.*, 1988; Sun *et al.*, 2012).

A major signal underlying maturation of the Sertoli cell and initiation of spermatogenesis at puberty is the increase in intra-testicular testosterone content produced by the rise in gonadotrophin secretion at this stage of development. Whereas thyroid hormone is essential for the normal timing of Sertoli cell maturation (Wagner *et al.*, 2008), the action of this hormone within the testis has been considered to be permissive and not to be linked to gonadotrophin action. This view may now need to be modified in light of the argument above that thyroid hormone activity of the testis, like that of androgen status, also may be actively regulated at the time of puberty. In the case of the primate, it now seems reasonable to posit that increased thyroid hormone activity in the testis at the end of juvenile development and the ensuing pubertal initiation of Sertoli cell maturation is driven, at least in part, by gonadotrophin-dependent changes in the expression of testicular miRNAs that regulate *DIO2* and *DIO3* to favor increased thyroid hormone activity. Whether the gonadotrophin-dependent changes in androgenicity and thyroid hormone activity within the testis at the onset of puberty occur in parallel or in series remain to be explored.

The X chromosome of the monkey was found to encode 97 precursor miRNAs from which five mature miRNAs, including miR-221-3p, were differentially expressed after gonadotrophin treatment. Although mir-221 and mir-222 are transcribed from the same promoter, only miR-221-3p was found to be up-regulated. Previously, expression of these two miRNAs was shown to be restricted to undifferentiated spermatogonia in the mouse and to maintain these cells in an undifferentiated state by inhibiting the translation of c-KIT, a promoter of spermatogonia differentiation (Yang *et al.*, 2013). The function of miR-221-3p in the present primate model, however, is unclear because we have previously shown that 48 h of gonadotrophin stimulation resulted in undifferentiated A spermatogonia committing to a path of differentiation.

Two other induced miRNAs derived from the X chromosome are potential facilitators of cell differentiation in the testis. miR-223 inhibited growth and promoted apoptosis via mechanistic target of rapamycin (mTOR) in hepatocellular carcinoma cell culture models (Dong *et al.*, 2017). Interestingly, the mTOR complex is required for the proliferation and differentiation of undifferentiated spermatogonia in mice (Serra *et al.*, 2017). miR-503 inhibited cell proliferation (Jiang *et al.*, 2017) and promoted monocyte and cardiomyocyte differentiation (Forrest *et al.*, 2010; Shen *et al.*, 2016), but no direct link to the differentiation of testis cells has been established yet. The gonadotrophin-induced changes in expression of the final two differentially expressed X-linked miRNAs are predicted to inhibit cell proliferation. The up-regulated miR-188-5p suppressed the G1/S transition and cell proliferation by inhibiting multiple cyclin/cyclin-dependent kinase complexes and the Rb/E2F pathway (Wu *et al.*, 2014). miR-450b-3p, which was down-regulated, was shown to decrease the proliferation of lung cancer cells by targeting interferon regulatory factor 2 (Liu *et al.*, 2016).

Of the differentially expressed miRNAs that were encoded on chromosomes other than X, down-regulated miR-190b and up-regulated miR-671-5p were previously found to be expressed predominately in mouse spermatogonial stem cells (Tan *et al.*, 2014) raising the possibility that these miRNAs in the monkey testis are associated with regulating the behavior of undifferentiated Type A spermatogonia following gonadotrophin stimulation.

Finally, miR-494, which was induced by gonadotrophin in the present study, has been associated with tumor aggressiveness and metastasis of colorectal cancer and the promotion of cell migration and invasion by inhibiting the expression of phosphatase and tensin homolog deleted on chromosome 10 (PTEN) (Sun *et al.*, 2014). Because the loss of PTEN activity promotes the production of differentiating spermatogonia in mice (Zhou *et al.*, 2015), it is possible that up-regulation of miR-494 by gonadotrophin stimulation may decrease PTEN levels and facilitate the initial differentiation of Type A spermatogonia. Other miRNAs regulated by gonadotrophin stimulation of the juvenile monkey testis have been implicated as tumor suppressors, including down-regulated miR-1247-5p as well as up-regulated miR-485-3p and miR-370-5p (Kim *et al.*, 2014; Zhou *et al.*, 2016; Wu *et al.*, 2017). Together, these data provide new potential mechanisms by which gonadotrophin-mediated changes in miRNA expression could regulate the proliferation and differentiation of Ad and Ap spermatogonia (or somatic testicular cells) during the initiation of spermatogenesis at the time of puberty in higher primates.

Although nearly 400 small RNAs (predominantly snoRNAs) were identified in the testis of the vehicle-treated monkeys, only 16 (12 snoRNA and four snRNA) transcripts were differentially expressed after gonadotrophin stimulation. All of the differentially expressed snoRNAs were members of the C/D box class called SNORDs that contain the conserved sequence motifs known as the C box (UGAUGA) and the D box (CUGA) (Dupuis-Sandoval *et al.*, 2015), and six belonged to a cluster of gene repeats located in an imprinted region on chromosome 7 that is associated with Prader–Willi syndrome. SNORDs were first recognized as regulators of rRNAs, but recent studies have demonstrated that they also regulate pre-mRNA alternative splicing, mRNA abundance and enzyme activity and may be processed into shorter non-coding RNAs resembling miRNAs and piwi-interacting RNAs (Falaleeva *et al.*, 2017).

Gonadotrophin stimulation of the juvenile monkey testis resulted in an 84% decrease in the level of *SNORD33*, that is considered to inhibit the propagation of oxidative stress (Michel *et al.*, 2011). In concordance with the dramatic gonadotrophin-induced repression of this transcript, several mRNAs associated with the oxidative stress response and detoxification were previously shown to be up-regulated in the same testes (Ramaswamy *et al.*, 2017). Because oxidative stress and reactive oxygen species (ROS) promote the differentiation of spermatogonial stem cells (Morimoto *et al.*, 2013, 2015), the observed decrease in *SNORD33* expression may be a gonadotrophin-induced adaptive response that would maintain ROS at levels favoring the differentiation of undifferentiated Type A spermatogonia.

Five copies of SNORD116, an orphan SNORD with no predictable rRNA targets, were markedly up-regulated by gonadotrophin stimulation. Although *SNORD116* can regulate over 200 transcripts (Falaleeva *et al.*, 2015) including the genes encoding chloride voltage-gated channel Kb and semaphorin3B that we previously reported to be down-regulated by at least 50% after gonadotrophin stimulation of the juvenile monkey testis (Ramaswamy *et al.*, 2017), the functional significance of this relationship in the present context is not understood because the induced transcripts accounted for <10% of all *SNORD116* expression from 29 copies of the gene.

SNORD115 is known to regulate the expression of 10 mRNAs and amplify the actions of *SNORD116* (Falaleeva *et al.*, 2015). *SNORD115* also was the first SNORD shown to regulate alternative splicing, including splice site selection of serotonin receptor 2 C (Kishore and Stamm, 2006) as well as the dolichyl-phosphate mannosyltransferase subunit 2, regulatory, TATA-box binding protein associated factor 1, Ral GEF with PH domain and SH3 binding motif 1, polybromo 1, and corticotropin releasing hormone receptor 1 mRNAs (Kishore *et al.*, 2010). However, the testicular functions remain unknown for the three down-regulated copies of *SNORD115* and the poorly characterized *SNORD49* and *SNORD103*, whose levels were reduced by >99 and 65%, respectively, after gonadotrophin treatment.

In summary, using testicular RNA obtained from the vehicle- and gonadotrophin-treated (48 h) juvenile rhesus monkeys previously reported (Ramaswamy *et al.*, 2017), we now provide the first description of the miRNA and other small RNA testicular transcriptomes of the juvenile monkey. We also identity 51 transcripts from these two classes of RNA that are up- or down-regulated in response to a mode of gonadotrophin stimulation previously established to trigger the commitment by undifferentiated Type A spermatogonia to proceed down the path of differentiation (Ramaswamy *et al.*, 2017). A large portion of the gonadotrophin-induced, differentially expressed miRNAs were derived from the *DLK1-DIO3* locus that is known to regulate self-renewal and differentiation, suggesting that the miRNAs from this region may target pioneer factors contributing to the fate of Type A undifferentiated spermatogonia. The finding that gonadotrophin-induced changes in the expression of four miRNA transcripts predicted to target *DIO2* and *DIO3* to favor increased thyroid hormone activity in the testis, together with the recognition that expression of several thyroid hormone target genes were changed concomitantly, lead us to posit that the primate testis is held in a state of low thyroid hormone activity prior to puberty. We further hypothesize that this posited low thyroid activity of the primate testis during juvenile development is necessary to maintain the proliferation of Sertoli cells throughout the pre-pubertal years.

With the onset of puberty, an increase in gonadotrophin secretion is argued to result in an increase in thyroid hormone activity in the testis that, together with an increase in intra-testicular androgen content, leads to differentiation of the Sertoli cell and the initiation of spermatogenesis that begins with the differentiation of Type A spermatogonia.

Supplementary data

Supplementary data are available at *Molecular Human Reproduction* online.

Acknowledgments

We should like to acknowledge that this study would not have been possible without Dr. Suresh Ramaswamy, who conducted the in vivo experiments that generated the material used in this study. We thank Dr. Will MacDonald and Ms Abby Neiser (University of Pittsburgh, Magee Womens Research Institute) for assistance in mapping imprinted methylation domains and performing RT-qPCR assays, respectively. Portions of this report were presented previously in poster format at the 2015 and 2018 meetings of the Society for the Study of Reproduction.

Authors' roles

P.A played a major role in describing the testicular small RNA transcriptome and conducting pathway analysis and contributed to data analysis and writing the manuscript. R.S. conducted the pipeline analysis of the RNA-Seq data. A.B. provided support and funding for PA, contributed to discussion of results and read and edited manuscript. U.R.C. directed the pipeline analysis of the RNA-Seq data and contributed to developing strategies for sequence analysis and data mining. T.M.P. is responsible for overall experimental design, obtaining financial support to conduct the study, and guaranteeing that the experiments were conducted in accord with NIH and University of Pittsburgh guidelines for the care and treatment of experimental animals, assisted with all surgical procedures, guided strategy for data analysis and presentation and is a co-principal writer of the manuscript. W.H.W. is responsible for pathway analysis and overall mining of the RNA-Seq data, performed RT-qPCR analyses, is a co-principal writer of the manuscript and provided final approval for submission of the paper.

Funding

National Institutes of Health (NIH) (RO1-HD072189-01 to T.M.P.); Endocrine Society Summer Research Fellowship Award and Consejo Nacional de Investigaciones Científicas y Técnicas (CONICET, Argentine Research Council) to P.A.

Conflict of interest

None declared.

References

Agarwal V, Bell GW, Nam JW, Bartel DP. Predicting effective microRNA target sites in mammalian mRNAs. *Elife* 2015;**4**:e05005.

Anders S, Pyl PT, Huber W. HTSeq—a Python framework to work with high-throughput sequencing data. *Bioinformatics* 2015;**31**:166–169.

Bookout AL, Cummins CL, Mangelsdorf DJ, Pesola JM, Kramer MF. High-throughput real-time quantitative reverse transcription PCR. *Curr Prot Mol Biol*. 2006;**73**:15.8.1–15.8.28

Bungay A, Selden C, Brown D, Malik R, Hubank M, Hodgson H. Microarray analysis of mitogenic effects of T3 on the rat liver. *J Gastroenterol Hepatol* 2008;**23**:1926–1933.

Bunick D, Kirby J, Hess RA, Cooke PS. Developmental expression of testis messenger ribonucleic acids in the rat following propylthiouracil-induced neonatal hypothyroidism. *Biol Reprod* 1994;**51**:706–713.

Castro-Magana M, Angulo M, Canas A, Sharp A, Fuentes B. Hypothalamic-pituitary gonadal axis in boys with primary hypothyroidism and macro-orchidism. *J Pediatr* 1988;**112**:397–402.

Chen J, Cai T, Zheng C, Lin X, Wang G, Liao S, Wang X, Gan H, Zhang D, Hu X *et al*. MicroRNA-202 maintains spermatogonial stem cells by inhibiting cell cycle regulators and RNA binding proteins. *Nucleic Acids Res* 2017;**45**:4142–4157.

Dentice M, Marsili A, Zavacki A, Larsen PR, Salvatore D. The deiodinases and the control of intracellular thyroid hormone signaling during cellular differentiation. *Biochim Biophys Acta* 2013;**1830**:3937–3945.

Dong Z, Qi R, Guo X, Zhao X, Li Y, Zeng Z, Bai W, Chang X, Hao L, Chen Y *et al*. MiR-223 modulates hepatocellular carcinoma cell proliferation through promoting apoptosis via the Rab1-mediated mTOR activation. *Biochem Biophys Res Commun* 2017;**483**:630–637.

Dupuis-Sandoval F, Poirier M, Scott MS. The emerging landscape of small nucleolar RNAs in cell biology. *Wiley Interdiscip Rev RNA* 2015;**6**:381–397.

Falaleeva M, Surface J, Shen M, de la Grange P, Stamm S. SNORD116 and SNORD115 change expression of multiple genes and modify each other's activity. *Gene* 2015;**572**:266–273.

Falaleeva M, Welden JR, Duncan MJ, Stamm S. C/D-box snoRNAs form methylating and non-methylating ribonucleoprotein complexes: Old dogs show new tricks. *Bioessays* 2017;**39**:6, 1600264.

Forrest AR, Kanamori-Katayama M, Tomaru Y, Lassmann T, Ninomiya N, Takahashi Y, de Hoon MJ, Kubosaki A, Kaiho A, Suzuki M *et al*. Induction of microRNAs, mir-155, mir-222, mir-424 and mir-503, promotes monocytic differentiation through combinatorial regulation. *Leukemia* 2010;**24**:460–466.

Friedlander MR, Mackowiak SD, Li N, Chen W, Rajewsky N. miRDeep2 accurately identifies known and hundreds of novel microRNA genes in seven animal clades. *Nucleic Acids Res* 2012;**40**:37–52.

Fujimoto N, Kitamura S, Uramaru N, Miyagawa S, Iguchi T. Identification of hepatic thyroid hormone-responsive genes in neonatal rats: Potential targets for thyroid hormone-disrupting chemicals. *Toxicol Lett* 2018;**286**:48–53.

Huang YH, Chin CC, Ho HN, Chou CK, Shen CN, Kuo HC, Wu TJ, Wu YC, Hung YC, Chang CC *et al*. Pluripotency of mouse spermatogonial stem cells maintained by IGF-1- dependent pathway. *FASEB J* 2009;**23**:2076–2087.

Jiajie T, Yanzhou Y, Hoi-Hung AC, Zi-Jiang C, Wai-Yee C. Conserved miR-10 family represses proliferation and induces apoptosis in ovarian granulosa cells. *Sci Rep* 2017;**7**:41304.

Jiang L, Zhao Z, Zheng L, Xue L, Zhan Q, Song Y. Downregulation of miR-503 Promotes ESCC Cell Proliferation, Migration, and Invasion by Targeting Cyclin D1. *Genomics Proteomics Bioinformatics* 2017;**15**:208–217.

Jung YH, Gupta MK, Shin JY, Uhm SJ, Lee HT. MicroRNA signature in testes-derived male germ-line stem cells. *Mol Hum Reprod* 2010;**16**:804–810.

Kim JG, Kim TO, Bae JH, Shim JW, Kang MJ, Yang K, Ting AH, Yi JM. Epigenetically regulated MIR941 and MIR1247 target gastric cancer cell growth and migration. *Epigenetics* 2014;**9**:1018–1030.

Kishore S, Khanna A, Zhang Z, Hui J, Balwierz PJ, Stefan M, Beach C, Nicholls RD, Zavolan M, Stamm S. The snoRNA MBII-52 (SNORD 115)

is processed into smaller RNAs and regulates alternative splicing. *Hum Mol Genet* 2010;**19**:1153–1164.

Kishore S, Stamm S. The snoRNA HBII-52 regulates alternative splicing of the serotonin receptor 2C. *Science* 2006;**311**:230–232.

Kozomara A, Griffiths-Jones S. miRBase: annotating high confidence microRNAs using deep sequencing data. *Nucleic Acids Res* 2014;**42**: D68–D73.

Langmead B, Trapnell C, Pop M, Salzberg SL. Ultrafast and memory-efficient alignment of short DNA sequences to the human genome. *Genome Biol* 2009;**10**:R25.

Liu L, Luo GZ, Yang W, Zhao X, Zheng Q, Lv Z, Li W, Wu HJ, Wang L, Wang XJ *et al*. Activation of the imprinted Dlk1-Dio3 region correlates with pluripotency levels of mouse stem cells. *J Biol Chem* 2010;**285**: 19483–19490.

Liu F, Yu X, Huang H, Chen X, Wang J, Zhang X, Lin Q. Upregulation of microRNA-450 inhibits the progression of lung cancer in vitro and in vivo by targeting interferon regulatory factor 2. *Int J Mol Med* 2016;**38**: 283–290.

Mann DR, Akinbami MA, Gould KG, Castracane VD. Leptin and thyroxine during sexual development in male monkeys: effect of neonatal gonadotropin-releasing hormone antagonist treatment and delayed puberty on the developmental pattern of leptin and thyroxine secretion. *Eur J Endocrinol* 2002;**146**:891–898.

Martinez ME, Karaczyn A, Stohn JP, Donnelly WT, Croteau W, Peeters RP, Galton VA, Forrest D St, Germain D, Hernandez A. The Type 3 Deiodinase Is a Critical Determinant of Appropriate Thyroid Hormone Action in the Developing Testis. *Endocrinology* 2016;**157**:1276–1288.

Michel CI, Holley CL, Scruggs BS, Sidhu R, Brookheart RT, Listenberger LL, Behlke MA, Ory DS, Schaffer JE. Small nucleolar RNAs U32a, U33, and U35a are critical mediators of metabolic stress. *Cell Metab* 2011;**14**: 33–44.

Moradi S, Sharifi-Zarchi A, Ahmadi A, Mollamohammadi S, Stubenvoll A, Gunther S, Salekdeh GH, Asgari S, Braun T, Baharvand H. Small RNA Sequencing Reveals Dlk1-Dio3 Locus-Embedded MicroRNAs as Major Drivers of Ground-State Pluripotency. *Stem Cell Reports* 2017;**9**:2081–2096.

Morimoto H, Iwata K, Ogonuki N, Inoue K, Atsuo O, Kanatsu-Shinohara M, Morimoto T, Yabe-Nishimura C, Shinohara T. ROS are required for mouse spermatogonial stem cell self-renewal. *Cell Stem Cell* 2013;**12**: 774–786.

Morimoto H, Kanatsu-Shinohara M, Shinohara T. ROS-Generating Oxidase Nox3 Regulates the Self-Renewal of Mouse Spermatogonial Stem Cells. *Biol Reprod* 2015;**92**:147.

Niu Z, Goodyear SM, Rao S, Wu X, Tobias JW, Avarbock MR, Brinster RL. MicroRNA-21 regulates the self-renewal of mouse spermatogonial stem cells. *Proc Natl Acad Sci USA* 2011;**108**:12740–12745.

Orth JM. Proliferation of Sertoli cells in fetal and postnatal rats: a quantitative autoradiographic study. *Anat Rec* 1982;**203**:485–492.

Ortogero N, Hennig GW, Langille C, Ro S, McCarrey JR, Yan W. Computer-assisted annotation of murine Sertoli cell small RNA transcriptome. *Biol Reprod* 2013;**88**:3.

Plant TM, Ramaswamy S, Simorangkir D, Marshall GR. Postnatal and pubertal development of the rhesus monkey (Macaca mulatta) testis. *AnnNYAcadSci* 2005;**1061**:149–162.

Plant TM, Terasawa E, Witchel SF. Puberty in non-human Primates and Man. In: Plant TM, Zeleznick AJ (eds). *Physiology of Reproduction*. London, England: Elsevier, 2015:1487–1536.

Qian P, He XC, Paulson A, Li Z, Tao F, Perry JM, Guo F, Zhao M, Zhi L, Venkatraman A *et al*. The Dlk1-Gtl2 Locus Preserves LT-HSC Function by Inhibiting the PI3K-mTOR Pathway to Restrict Mitochondrial Metabolism. *Cell Stem Cell* 2016;**18**:214–228.

Ramaswamy S, Walker WH, Aliberti P, Sethi R, Marshall GR, Smith A, Nourashrafeddin S, Belgorosky A, Chandran UR, Hedger MP *et al*. The testicular transcriptome associated with spermatogonia differentiation initiated by gonadotrophin stimulation in the juvenile rhesus monkey (Macaca mulatta). *Hum Reprod* 2017;**32**:2088–2100.

Ramos S, Goya L, Alvarez C, Pascual-Leone AM. Mechanism of hypothyroidism action on insulin-like growth factor-I and -II from neonatal to adult rats: insulin mediates thyroid hormone effects in the neonatal period. *Endocrinology* 1998;**139**:4782–4792.

Rijntjes E, Swarts HJ, Anand-Ivell R, Teerds KJ. Prenatal induced chronic dietary hypothyroidism delays but does not block adult-type Leydig cell development. *Am J Physiol Endocrinol Metab* 2009;**296**:E305–E314.

Robinson MD, McCarthy DJ, Smyth GK. edgeR: a Bioconductor package for differential expression analysis of digital gene expression data. *Bioinformatics* 2010;**26**:139–140.

Robinson JT, Thorvaldsdottir H, Winckler W, Guttman M, Lander ES, Getz G, Mesirov JP. Integrative genomics viewer. *Nat Biotechnol* 2011; **29**:24–26.

Rybak A, Fuchs H, Smirnova L, Brandt C, Pohl EE, Nitsch R, Wulczyn FG. A feedback loop comprising lin-28 and let-7 controls pre-let-7 maturation during neural stem-cell commitment. *Nat Cell Biol* 2008;**10**:987–993.

Seitz H, Royo H, Bortolin ML, Lin SP, Ferguson-Smith AC, Cavaille J. A large imprinted microRNA gene cluster at the mouse Dlk1-Gtl2 domain. *Genome Res* 2004;**14**:1741–1748.

Serra ND, Velte EK, Niedenberger BA, Kirsanov O, Geyer CB. Cell-autonomous requirement for mammalian target of rapamycin (Mtor) in spermatogonial proliferation and differentiation in the mousedagger. *Biol Reprod* 2017;**96**:816–828.

Shen X, Soibam B, Benham A, Xu X, Chopra M, Peng X, Yu W, Bao W, Liang R, Azares A *et al*. miR-322/-503 cluster is expressed in the earliest cardiac progenitor cells and drives cardiomyocyte specification. *Proc Natl Acad Sci USA* 2016;**113**:9551–9556.

Simorangkir DR, Ramaswamy S, Marshall GR, Roslund R, Plant TM. Sertoli cell differentiation in rhesus monkey (Macaca mulatta) is an early event in puberty and precedes attainment of the adult complement of undifferentiated spermatogonia. *Reproduction* 2012;**143**:513–522.

St Germain DL, Galton VA. The deiodinase family of selenoproteins. *Thyroid* 1997;**7**:655–668.

Sun Y, Bak B, Schoenmakers N, van Trotsenburg AS, Oostdijk W, Voshol P, Cambridge E, White JK, le Tissier P, Gharavy SN *et al*. Loss-of-function mutations in IGSF1 cause an X-linked syndrome of central hypothyroidism and testicular enlargement. *Nat Genet* 2012;**44**:1375–1381.

Sun HB, Chen X, Ji H, Wu T, Lu HW, Zhang Y, Li H, Li YM. miR494 is an independent prognostic factor and promotes cell migration and invasion in colorectal cancer by directly targeting PTEN. *Int J Oncol* 2014;**45**: 2486–2494.

Tan T, Zhang Y, Ji W, Zheng P. miRNA signature in mouse spermatogonial stem cells revealed by high-throughput sequencing. *Biomed Res Int* 2014; **2014**:154251.

Van Haaster LH, De Jong FH, Docter R, De Rooij DG. The effect of hypothyroidism on Sertoli cell proliferation and differentiation and hormone levels during testicular development in the rat. *Endocrinology* 1992;**131**: 1574–1576.

Van Haaster LH, De Jong FH, Docter R, De Rooij DG. High neonatal triiodothroneine levels reduce the period of Sertoli cell proliferation and accelerate tubular lumen formation in the rat testis and increase inhibin levels. *Endocrinology* 1993;**133**:755–760.

Wagner MS, Wajner SM, Maia AL. The role of thyroid hormone in testicular development and function. *JEndocrinol* 2008;**199**:351–365.

Weber JE, Turner TT, Tung KS, Russell LD. Effects of cytochalasin D on the integrity of the Sertoli cell (blood-testis) barrier. *Am J Anat* 1988; **182**:130–147.

Wood MA, Mukherjee P, Toocheck CA, Walker WH. Upstream stimulatory factor induces Nr5a1 and Shbg gene expression during the onset of rat Sertoli cell differentiation. *Biol Reprod* 2011;**85**:965–976.

Wu J, Li J, Ren J, Zhang D. MicroRNA-485-5p represses melanoma cell invasion and proliferation by suppressing Frizzled7. *Biomed Pharmacother* 2017;**90**:303–310.

Wu J, Lv Q, He J, Zhang H, Mei X, Cui K, Huang N, Xie W, Xu N, Zhang Y. MicroRNA-188 suppresses G1/S transition by targeting multiple cyclin/CDK complexes. *Cell Commun Signal* 2014;**12**:66.

Yang QE, Racicot KE, Kaucher AV, Oatley MJ, Oatley JM. MicroRNAs 221 and 222 regulate the undifferentiated state in mammalian male germ cells. *Development* 2013;**140**:280–290.

Zhou W, Shao H, Zhang D, Dong J, Cheng W, Wang L, Teng Y, Yu Z. PTEN signaling is required for the maintenance of spermatogonial stem cells in mouse, by regulating the expressions of PLZF and UTF1. *Cell Biosci* 2015;**5**:42.

Zhou H, Zhang M, Yuan H, Zheng W, Meng C, Zhao D. MicroRNA-154 functions as a tumor suppressor in osteosarcoma by targeting Wnt5a. *Oncol Rep* 2016;**35**:1851–1858.